# Meson retardation, three-body forces, and medium modifications to the nucleon-nucleon interaction

Mikkel B. Johnson
*Los Alamos National Laboratory, Los Alamos, New Mexico 87545*

J. Haidenbauer and Karl Holinde
*Institut für Kernphysik der Forschungszentrum Jülich G.m.b.H., D-5170 Jülich, West Germany*
(Received 23 July 1990)

We critically examine two formally equivalent approaches to the many-body problem, one of which is based on an effective energy-dependent interaction and the other on an effective energy-independent interaction (an instantaneous, but nonlocal, potential). The interactions are mediated by the same set of mesons, with common masses, coupling constants, and form factors, and they give similar reproductions of the two-body data. We examine the higher-order contributions in the many-body theory, and we are able to identify specific ingredients that could lead to different rates of convergence for the different interactions. For the three-body system, we find an important contribution to the three-body force that is large in the energy-dependent interaction and nearly cancels out of the instantaneous potential. For the many-body system we find numerous density-dependent terms that contribute to the energy-dependent interaction but not to the instantaneous one. We show numerical results for the binding energy per particle of nuclear matter based on the solution of the two-body Bethe-Goldstone equation. We find substantially less binding for the instantaneous potential, thus observing that in actual calculations the many-body theory converges at a different rate for the two types of interaction. We conclude that nuclear matter properties can be calculated with more reliability and less computational effort for the case of the instantaneous potential.

## I. INTRODUCTION

In recent years, numerous meson-theoretical nucleon-nucleon interactions $V$ have been proposed. As a rule, these reproduce quite well the nucleon-nucleon phase shifts below the meson-production threshold once the meson-nucleon couplings are appropriately adjusted. The interactions are sometimes taken to depend on the asymptotic energy $E$ of the two nucleons [so $V=V(E)$], as in the case of some versions of the Bonn interaction,[1] and sometimes taken to be instantaneous, in which case $V$ is energy independent but nonlocal, and can be derived from the folded-diagram expansion.[2] Below the meson-production threshold, both forms are, in principle, equally valid representations of the interaction and can be systematically derived from an underlying meson theory in versions of the Brillouin-Wigner and Rayleigh-Schrödinger perturbation theories, respectively. Recently,[3] we showed that equivalently good representations of the on-shell nucleon-nucleon scattering data could be obtained with both instantaneous and energy-dependent interactions using the same set of mesons with the same couplings to nucleons. It was thereby demonstrated that, in the two-body sector, retardation, arising naturally as a result of the meson exchange, could be described equally well, in practice, through an explicit dependence on $E$, or alternatively, in the instantaneous potential, as a folded diagram.

In this paper, we want to extend our investigations to the case of systems consisting of three (and more) nucleons. We would like to know whether the practical equivalence observed for two nucleons also holds in the many-body system. Specifically, we will investigate whether the binding energy per particle BE/$A$ of infinite nuclear matter can be calculated with comparable feasibility in both schemes, or whether one scheme is definitely superior and hence preferred as a technique for testing meson-theoretical models.

Observables for such systems are calculated with the help of the Goldstone linked-cluster expansion.[4] In principle, expansions in both schemes ultimately lead to the same value for BE/$A$ if they are derived from the same meson theory as in our work. To obtain a reliable result in practice, however, one scheme may require the evaluation of many more terms in the corresponding perturbation expansion. The main issue is then to decide which expansion is likely to be more convergent, and, moreover, in which scheme the terms of the expansion can be more easily evaluated.

In general, there are two types of complications to be expected when going from the two-body to the many-body system. First, density-dependent modifications of the two-body force have to be considered. Secondly, genuine three- and higher-body forces appear in the perturbation expansion. It will turn out that the instantaneous potential approach is definitely simpler and hence preferred. One reason is that density-dependent corrections simply do not arise in this case, so that there are fewer terms to be evaluated. With the extra effort that is required to calculate the density-dependent terms, the

 

energy-dependent scheme has no obvious justification, at least at this time. Additionally, we find, in contrast to the energy-dependent interaction, that there are strong cancellations among the various pieces of the three-body force considered for the instantaneous potential, which would appear to reduce the effort needed to make the calculation and enhance the apparent rate of convergence in this case.

In Sec. II we present and discuss the meson-theory model on which our calculations are based. In Sec. III we formally examine the structure of the effective interactions in the energy-dependent and instantaneous schemes. We show that the structure of the forces, the nature of the density-dependent corrections, and the interplay between the various terms are quite different in the two cases.

In Sec. IV we illustrate the theory by studying an important set of three-body forces. We show that there are strong cancellations between two types of folded diagrams occurring in this set, and that these cancellations have no counterpart in the energy-dependent scheme. These three-body forces help explain different numerical results that have been found in previous calculations of the triton binding energy using energy-dependent and energy-independent interactions; in particular, we show that the equivalence between the two schemes is satisfied when these three-body forces are included.

In Sec. V we give numerical results for nuclear matter, showing that $BE/A$ is *not* the same when the Goldstone expansion is truncated at the two-body level, even for two-body forces that are constructed from the same meson theory and give the same nucleon-nucleon phase shifts. We argue that the differences are a consequence of the omission of three-body clusters and the neglect of various many-body terms and density-dependent additions to the two-body interaction identified in Sec. III. Three-body clusters and three-body forces are estimated for the instantaneous potential, but additional numerical calculations for the energy-dependent scheme are required to fully establish the equivalence between the two approaches for nuclear matter.

In Sec. VI we summarize our results and draw conclusions. Our main conclusion is that the instantaneous potential approach is preferable based on the criterion of simplicity.

## II. MESON-THEORETICAL TWO-BODY MODEL

Our energy-dependent interaction, which we call OBEPT′, consists of single exchanges of $\pi$, $\eta$, $\rho$, $\omega$, $\sigma$, and $\delta$ mesons between nucleons. Antinucleons are omitted in the discussion presented here, which seems to be a good approximation, at least for pions with pseudovector coupling to nucleons.[5] We use exactly the same $\sigma$ meson in both isospin channels, in contrast to OBEPT in Ref. 1 (Table 8, Appendix B.2), where the parameters for the $\sigma$ meson are slightly different in the two channels. The masses, coupling constants, and cutoff masses $\Lambda_\alpha$ are shown in Table I; they have been determined by a fit to the two-body data. Results for the scattering phase shifts can be found in Ref. 3. It should be noted that the fit is as good as that for OBEPT; only the triplet $S$-wave scattering length $a_t$ is slightly inferior. (In fact, the isospin splitting in $\sigma$ exchange has been introduced in OBEPT just to obtain quantitative agreement with the empirical $a_t$ value.)

TABLE I. Parameters for the energy-dependent interaction OBEPT′, together with the modified scalar coupling constants (in parentheses) used for the corresponding instantaneous interaction. The number in square brackets denotes the tensor-to-vector coupling ratio. For the definition of the parameters, see Ref. 1.

| Meson | Mass (MeV) | $g_\alpha^2/4\pi$ | $\Lambda_\alpha$ (MeV) |
|---|---|---|---|
| $\pi$ | 138.0 | 14.40 | 1750 |
| $\eta$ | 548.8 | 5.00 | 1500 |
| $\sigma$ | 550.0 | 8.88 (8.7745) | 2000 |
| $\delta$ | 983.0 | 1.05 (0.1207) | 2000 |
| $\rho$ | 769.0 | 0.90 [6.1] | 1500 |
| $\omega$ | 782.6 | 20.00 | 1500 |

The corresponding folded-diagram potential consists of one-boson-exchange (OBE) terms for each of the mesons with the same masses, coupling constants, and form factors that were used in OBEPT′. However, to account for the retardation of the OBE potential, we must augment the potential by the two-pion-exchange folded diagram, as in Ref. 3. This diagram is also energy independent. We showed in Ref. 3 that these energy-dependent and instantaneous interactions give nearly the same on-shell results, which establishes that the theory is rapidly convergent.

In order to meaningfully compare the nuclear matter results of the energy-dependent and instantaneous potentials, we must consider the following point. If we find differences between the results, these could arise from omissions in the many-body sector, or from omissions of higher-order diagrams at the two-body level. In order to avoid confusing these two possibilities, we will next make small adjustments in the coupling constants of the scalar mesons (for the case of the instantaneous interaction) to give essentially exactly equivalent fits to the two-body data for the energy-dependent and instantaneous interactions. This adjustment compensates approximately for the omission of higher-order folded diagrams in the two-body force and may also reflect our omission of two-meson-exchange folded diagrams involving mesons heavier than pions. The results are also shown in Table I. The changes are basically very small, and one can see that the largest occurs in the short-range component (of the scalar $\delta$ meson). This is consistent with the results of Ref. 2, where it was pointed out that the retardation effects arising from energy dependence in a given order are naturally of short-range character because they can be represented as higher-order (folded) diagrams.

It is important to look a bit more carefully at the $^3S_1$-$^3D_1$ channel. In this channel one finds the tensor force, which has a major influence on the saturation of nuclear matter. The $\epsilon_1$ parameter for the energy-dependent OBEPT′ is shown in Fig. 1 along with the folded-diagram

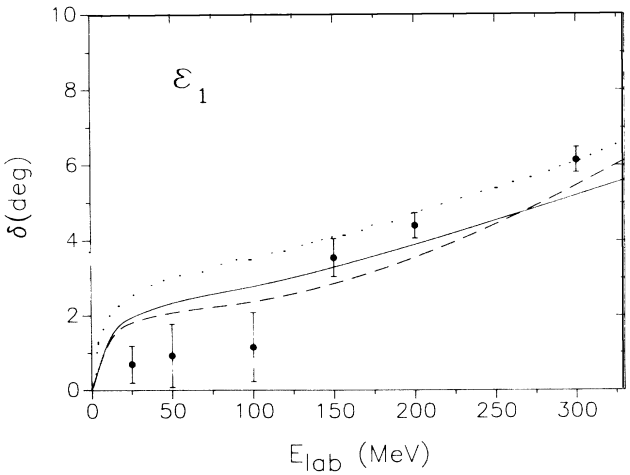


FIG. 1. Comparing experimental and theoretical values of the $\epsilon_1$ parameter. The dashed curve is OBEPT' and the dotted curve the corresponding folded-diagram potential. The solid curve is the calculation of the folded-diagram potential corresponding to the modified scalar-meson coupling constants in Table I.

potentials corresponding to the two sets of parameters in Table I. We see that all of these look quite good compared to the empirical data. The deuteron properties are shown in Table II. For our purposes, it is important that the deuteron binding energy is the same for both interactions; the eigenvalues of bound states are, in any case, supposed to be preserved in the transformation from the underlying Hamiltonian to the instantaneous potential by folded diagrams.[10]

The fact that the quadrupole moment is not the same for the two cases in Table II reflects the need for specific corrections in both schemes. For the energy-dependent interaction, these have been discussed by Chemtob and Rho,[6] who point out two sources for them. One is associated with the wave-function normalization, and the other is a piece of the exchange current, the so-called meson-in-flight term. The former is known to give rise to a decrease in the value of $Q$ by about 4%, but the latter have, to our knowledge, never been evaluated. In the instantaneous potential approach there is no wave-function normalization correction, but the analog of meson-in-flight corrections does arise, and these can be calculated as an effective operator along the lines indicated in Ref. 2. As pointed out there, there are rather strong cancellations between two folded diagrams, so that the net effect is small. Thus, the difference between the two values of the quadrupole moment in Table II reflects the wave-function normalization and the meson-in-flight corrections corresponding to the energy-dependent interaction.

The percentage $D$ state is a special case. As for $Q$, it is different for the two interactions. However, in contrast to $Q$, there is no reason for this quantity to be the same, because the percentage $D$ state is not an observable. Desplanques[7] has shown that an increase in the percentage $D$ state by about the amount shown in Table II is a natural consequence of transforming from the energy-dependent to the equivalent energy-independent interaction.

## III. MANY-BODY THEORY

The energy-dependent scheme applied by the Bonn group[8] is an application of the formalism of Bloch and Horowitz.[9] The many-body theory for the instantaneous interaction is found in Ref. 2, which is an application of the general folded-diagram approach of Ref. 10. In order to understand the nature of the differences that we will find in triton binding-energy results and our nuclear matter calculations, the structure of these theories needs to be made more explicit in higher order. We will attempt to do this in the present section.

The study presented in this section will help us decide later whether the numerical differences that we find are of a trivial nature (e.g., arising simply as quantitative differences in the evaluation of the same algebraic expression), or whether they arise from deeper structural differences in the theory. From this we will be able to determine the answer to the question posed in the Introduction; namely, whether one of the two interaction schemes provides a decidely more economical basis for testing the many-body meson theory.

### A. Energy-dependent scheme

Bloch and Horowitz showed how to define an effective interaction $v(z)$ in a model space. They consider the resolvent operator $\kappa(z)=(z-H+i\eta)$, where $H=H_0+V$ is the full Hamiltonian of the system. Bloch and Horowitz use time-ordered perturbation theory, called "old-fashioned perturbation theory" in Ref. 8. In this case, any state $|i\rangle$ of the system is characterized globally as a many-body state containing $A$ nucleons and some number $(0,1,2,\ldots)$ of mesons. They introduce projec-

TABLE II. Deuteron data (energy $E_B$, quadrupole moment $Q$, and percentage $D$ state $P_D$), nuclear-matter properties (binding energy per particle BE/$A$ and saturation Fermi momentum $k_F$), and singlet and triplet scattering lengths ($a_s$,$a_t$) and effective ranges ($r_s$,$r_t$) for the energy-dependent interaction and instantaneous potential.

| Interaction | $E_B$ (MeV) | $Q$ (fm$^2$) | $P_D$ (%) | BE/$A$ (MeV) | $k_F$ (fm$^{-1}$) | $a_s$ (fm) | $r_s$ (fm) | $a_t$ (fm) | $r_t$ (fm) |
|---|---|---|---|---|---|---|---|---|---|
| Energy-dependent | 2.225 | 0.278 | 4.19 | 20.7 | 1.8 | −23.76 | 2.75 | 5.45 | 1.79 |
| Instantaneous | 2.225 | 0.298 | 5.97 | 11.3 | 1.5 | −23.83 | 2.75 | 5.44 | 1.78 |
| Experiment | 2.224 57 ±0.000 09 | 0.2860 ±0.0015 | | 16 ±0.5 | 1.36 ±0.05 | −23.7483 ±0.010 | 2.75 ±0.05 | 5.424 ±0.004 | 1.759 ±0.005 |

tion operators $P$ and $Q$ such that $P$ projects onto a state in the model space (in this case, any state with no mesons) and $Q$ projects onto any state outside the model space (a state with at least one meson). $v(z)$ is then an operator that has matrix elements between those states $|i\rangle$ for which $P|i\rangle$ does not vanish. $v(z)$ is given by the sum of all terms in the perturbation expansion of $\kappa(z)$ having only those intermediate states $|I\rangle$ for which $Q|I\rangle$ does not vanish. They show that for bound states the eigenvalues of the effective interaction of $H_0+v(z)$ are the same as the eigenvalues of the exact Hamiltonian $H$. For scattering states, one also obtains, in this fashion, the scattering $S$ matrix.

One can represent the matrix elements of $v(z)$ diagrammatically using usual many-body techniques, since $\kappa(z)$ is the Fourier transform of the time-evolution operator. The diagrams are usually called Feynman-Goldstone diagrams.

For the bound-state problem, the unperturbed Hamiltonian is the single-particle operator $H_0$,

$$H_0=T+U=\sum_i h_i \ , \tag{1}$$

where

$$h_i=t_i+u_i \ , \tag{2}$$

with $T$ being the kinetic-energy operator for the nucleons and $U$ being some suitably chosen single-particle potential. In this case, the perturbation would be $V-U$. The single-particle orbitals $|\phi_n\rangle$, which are eigenstates of $h$,

$$h|\phi_n\rangle=\epsilon_n|\phi_n\rangle \ , \tag{3}$$

correspond to either particles or holes in the Feynman-Goldstone diagrams. Holes may occupy only those states that belong to the "core" of the nucleus, the core being defined as all states whose energy lies below the Fermi energy $\epsilon_{FA}$. Particles occupy states whose energy is greater than $\epsilon_{FA}$.

In general, for the $A$-body system we will write the effective interaction as $v(\epsilon_{FA},z)$ to remind one that the individual terms contain medium modifications depending on the energy of its Fermi surface. This interaction contains terms of a zero-body, one-body, $n$-body character, so one may write

$$v(\epsilon_{FA},z)=\sum_n v^{(n)}(\epsilon_{FA},z) \ . \tag{4}$$

We will illustrate the contributions to $v$ below as Feynman-Goldstone diagrams. Feynman-Goldstone diagrams are time ordered, with particles propagating forward in time and holes backward in time. In our representation of these diagrams, time runs up. The terms are represented generically by a box; those with $n$ different from zero have $n$ external lines (legs) entering (or leaving) the box, as illustrated in Fig. 2. Each box connects $A$-particle states, but external legs with no interactions are not drawn. The external legs correspond to the case where valence particles or holes are added to the nucleus. When we omit $\epsilon_{FA}$ as an argument in $v$, we imply that all nucleon states characterizing $v(z)$ are particle states, as is appropriate to the two-body and perhaps other few-body systems. We next give examples of the boxes in Figs. 3–6. It is important to realize that the diagrams actually needed in a calculation are much greater in number than those shown; we generally just show one of many time orderings that contribute.

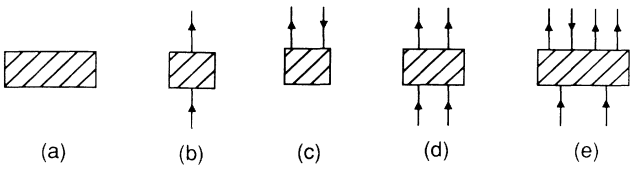


FIG. 2. Generic representation of diagrams contributing to Eq. (4).

Examples of the zero-body piece of the effective interaction $v^{(0)}(\epsilon_{FA},z)$ are shown in Fig. 3. This piece of the interaction gives the ground-state energy of a system containing no valence particles and holes. Recall that we omit antinucleons in this discussion, so that the lines running backward in time are holes. Figures 3(a)–(d) are two-hole-line clusters, and Fig. 3(e) is an example of a three-hole-line cluster. Figures 3(f) and (g) are examples of two-meson-exchange diagrams that have never, to our knowledge, been evaluated in nuclear-matter calculations.

The higher-order terms ($n>1$) $v^{(n)}(\epsilon_{FA},z)$ contribute to the interaction among valence particles and holes. Figure 4 shows some examples of the two-body contributions $v^{(2)}(\epsilon_{FA},z)$. In the free-space two-body interaction the diagrams with internal and external hole lines, e.g., Figs. 4(d)–(j), are absent, and there are, of course, no Pauli restrictions on the particle lines on the remaining diagrams.

Figures 4(d)–(g) are density-dependent contributions to the two-meson-exchange interaction, which have never, to our knowledge, been considered in nuclear-matter calculations. Figure 4(h)–(j) are examples of two-body interactions that act between particles and holes. Figure 4(j) is an off-diagonal piece that connects states with different numbers of particles and holes.

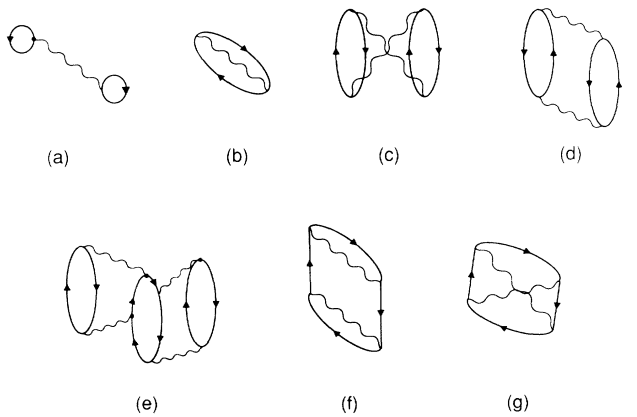


FIG. 3. Examples of connected clusters contributing to the zero-body piece of the effective energy-dependent interaction.

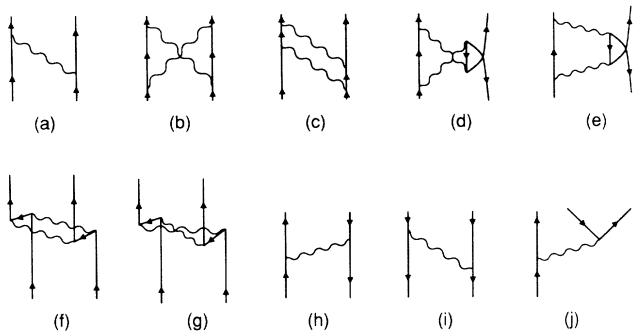


FIG. 4. Examples of linked clusters contributing to the two-body piece of the effective energy-dependent interaction.

Figure 5 gives examples of three-body interactions. Figure 5(a) is an example of the intrinsic three-body interaction. We use the term "intrinsic" to denote three-body diagrams that cannot be separated into two pieces by cutting a single internal nucleon line. Figures 5(b) and (c) are examples of the extrinsic three-body interaction, so called to distinguish it from the intrinsic terms. Extrinsic three-body forces tend to be specifically dependent on the particular representation used to account for retardation at the two-body level. Figure 5(d) is an example of a disconnected three-body interaction.

Examples of four-body interactions are shown in Fig. 6. Figure 6(a) is an intrinsic four-body interaction and Fig. 6(b) is an example of an extrinsic four-body interaction. Figure 6(b) is also an example of a disconnected four-body diagram.

One-body pieces $v^{(1)}(\epsilon_{FA},z)$ also exist, and those that occur in free space are related to nucleon self-energies, which are assumed to be adequately taken into account by the use of physical nucleon masses. This is, of course, only an expedient and not true as a general statement.

A fundamental problem with the pursuit of the Bloch-Horowitz expansion for $v^{(n)}(\epsilon_{FA},z)$ is that it contains disconnected diagrams. The existence of disconnected diagrams has been considered a drawback, and attempts to obtain a linked set of diagrams was one of the prime motivations for the invention of folded diagrams,[10,11] discussed below. In applications of the energy-dependent interaction to nuclear matter, this problem has been ignored. It is clear from the above discussion that the number of two-meson diagrams contributing to $v^{(n)}(\epsilon_{FA},z)$ is substantial; that is a practical drawback of the energy-dependent scheme.

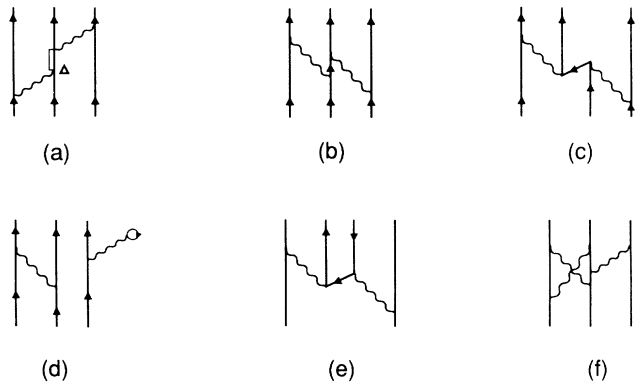


FIG. 5. Examples of linked clusters contributing to the three-body piece of the effective energy-dependent interaction. (a) is an intrinsic three-body force, (b)–(d) are examples of an extrinsic three-body interaction. (b) is an example of a disconnected cluster.

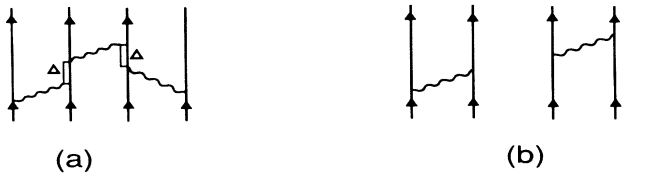


FIG. 6. Examples of linked-cluster contributions to the four-body piece of the effective energy-dependent interaction. (b) is an example of a disconnected cluster.

The theory of Ref. 8 deals with two cases. The first is the interaction of two free particles, so $A=2$ and no single-particle potential or Fermi energy is necessary to characterize the system. In that work, a restriction on the class of diagrams was imposed; namely, $v(z)$ was considered to consist only of two-body pieces, and these contained only the one-boson-exchange terms, which we denote $v^{(2)}_{\rm OBE}(z)$. Although just the lowest-order, one-boson-exchange pieces [e.g., Fig. 4(a)] were considered in Ref. 8, in subsequent applications consideration was given to the higher-order pieces of $v^{(2)}(z)$. For example, in some of the Bonn interaction studies, including the latest one,[1] two-meson-exchange pieces to $v^{(2)}(z)$, Figs. 4(b) and (c), were included.

The second case considered in Ref. 8 was infinite nuclear matter. The only property of nuclear matter studied was the binding energy; excited states were not considered. In this case there are no valence particles or holes and therefore the ground-state energy of the system is given by the sum of linked clusters, as in Fig. 2(a), which we have noted to constitute the zero-body piece of the effective interaction $v^{(0)}(\epsilon_{FA},z)$. In Ref. 8, the ladder of one-boson-exchange graphs was assumed to be the dominant element in the calculation of this two-hole-line cluster contribution to the ground-state energy. The individual "rungs" of this ladder are $v^{(2)}_{\rm OBE}(\epsilon_{FA},z)$, which are closely related to the free-space one-boson-exchange interaction $v^{(2)}_{\rm OBE}(z)$. They differ in the choice of the energy $z$, the choice of energies for the nucleon states [the existence of the potential $u$ in Eq. (2) arising from the presence of the other nucleons modifies the energies], and the Pauli restrictions on the intermediate states of $v^{(2)}(z)$ (particles and holes are defined differently depending upon the density). The summation of these ladders was accomplished by solving the Bethe-Goldstone equation.[4] Some calculations of the two-meson-exchange pieces of $v^{(2)}(\epsilon_{FA},z)$, Fig. 4(b) or (c), have also been obtained.[12]

If we are interested only in the ground-state binding energy of infinite nuclear matter, which is the many-body case studied in Ref. 8, it is only the zero-body piece of the

effective interaction $v^{(0)}(\epsilon_{FA},z)$ that enters, as we have stated. We also noted the observation of Ref. 8 that an important piece of this can be obtained by iterating $v^{(2)}(\epsilon_{FA},z)$. We point out here that this observation is actually quite general and that the entire operator $v^{(0)}(\epsilon_{FA},z)$ can be calculated by iterating the full effective interaction $v(z)$ as shown in Fig. 7. One only has to ensure that the individual terms $v^{(n)}(\epsilon_{FA},z)$ that are iterated lead to a connected set. In the two-body case of Ref. 8, this condition was automatically satisfied, but in higher order the classification becomes more intricate, because, as we have seen in Figs. 5 and 6, the individual terms $v^{(n)}(\epsilon_{FA},z)$ for $n>2$ may contain disconnected pieces. One may find the considerations of Ref. 13 to be of some value.

There is one final comment that we wish to make. One could try to define the effective interaction for the many-body system by constructing the diagrammatic expansion of $v^{(n)}(z)$ in the following sense: use the single-particle basis of Eq. (3), but treat all states as particle states. The advantage would be that the many medium modifications would disappear, affording some simplification to the bookkeeping. However, it becomes problematic to derive an appropriate linked-cluster expansion. The basic problem is to know how to fix $z$. We have found a way to circumvent this problem, but our result, although rather straightforward, is awkward to explain. In the end, we found the expansion just as complicated as $v^{(n)}(\epsilon_{FA},z)$.

Although ladders of terms $v^{(n)}(\epsilon_{FA},z)$ with $n$ different from 2 were not considered in Ref. 8, we will find it necessary to consider these higher-order terms in our work in order to identify the source of difference between the binding-energy results for the energy-dependent and energy-independent interactions. Therefore, we have generalized the results of Ref. 8 by carrying the Bloch-Horowitz scheme to higher order. This revealed certain undesirable features that did not show up in the lowest order considered in Ref. 8, as we have discussed. It is our feeling that these difficulties are inherent in the concept of an energy-dependent interaction and are not an artifact of the manner in which we have generalized from the results of Ref. 8.

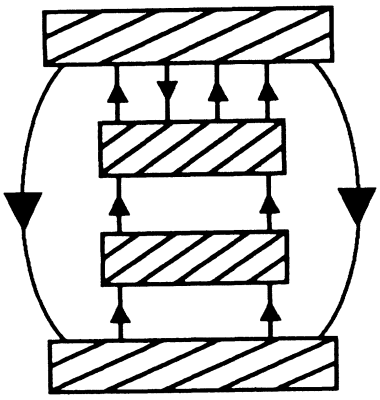

FIG. 7. Illustrating that zero-body connected clusters can be represented by iterations of interactions of the type shown in Figs. 3–5.

### B. Energy-independent interactions

The difficulty in finding a disconnected expansion for $v^{(n)}(\epsilon_{FA},z)$ is an old concern, and the consequences are discussed in the literature[14] in the context of the nonrelativistic many-body problem. Historically, searching for an alternative that would be connected led to the observation that elimination of the energy dependence automatically results in a linked-cluster expansion. Brandow, in Ref. 11, has shown this explicitly. In Ref. 10 it was shown how to simplify the procedure and arrive at the folded diagrams using time-dependent methods. The theory was later applied to the nucleon-nucleon interaction in Ref. 2. Next, we want to consider the extension of these results to the many-body system.

Results come out rather simple if the problem is set up in the following manner.[2] We define the states of the model space in terms of a suitable single-particle Hamiltonian [Eq. (3)]. The model space is taken to be spanned by the complete set of single-particle states for $A$ nucleons. Thus, all nucleon states are taken to be *active particle states* in the notation of Refs. 10 and 2. The passive states are then the meson states (we omit the antinucleons). The diagrams of the $A$-body problem are those for the time-evolution operator $U(+\infty,-\infty)$, each having $A$ incoming and $A$ outgoing lines. The results of Ref. 2 are sufficiently general so that they can be applied immediately to the many-body problem, even though the emphasis there was on the two-body problem.

Without further ado, we list the few lowest-order contributions to the two- and three-body force in the folded-diagram expansion. These are shown in Figs. 8 and 9, respectively. The folded diagram of the effective interaction $\overline{H}$ in Fig. 8(a) is the one-meson-exchange potential, and Figs. 8(b) and (c) constitute the two-meson-exchange potential. The horizontal solid line drawn in the diagrams is the time base and represents the time at which the diagram acts as an instantaneous potential. In all cases, the value of the diagram is found by integrating over all times subject to the constraint that the time base is fixed. The diagram in Fig. 8(b) is a model-correcting diagram and arises because the iteration of the one-meson-exchange potential, Fig. 8(a), includes some relative time orderings of the vertices that are not allowed in the two-meson-exchange ladder Feynman diagram. The model-correcting diagram is subtracted from the potential. The horizontal dashed lines in Fig. 8(b) are the time

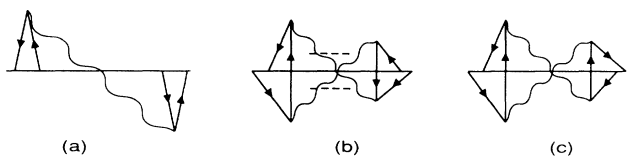


FIG. 8. Instantaneous two-body forces expressed in terms of folded diagrams. (a) is a single-box folded diagram and constitutes the one-meson-exchange potential, (b) a model-correcting double-box folded diagram. One additional term exists for which the role of the two nucleons is interchanged, (c) a true-correcting double-box folded diagram.

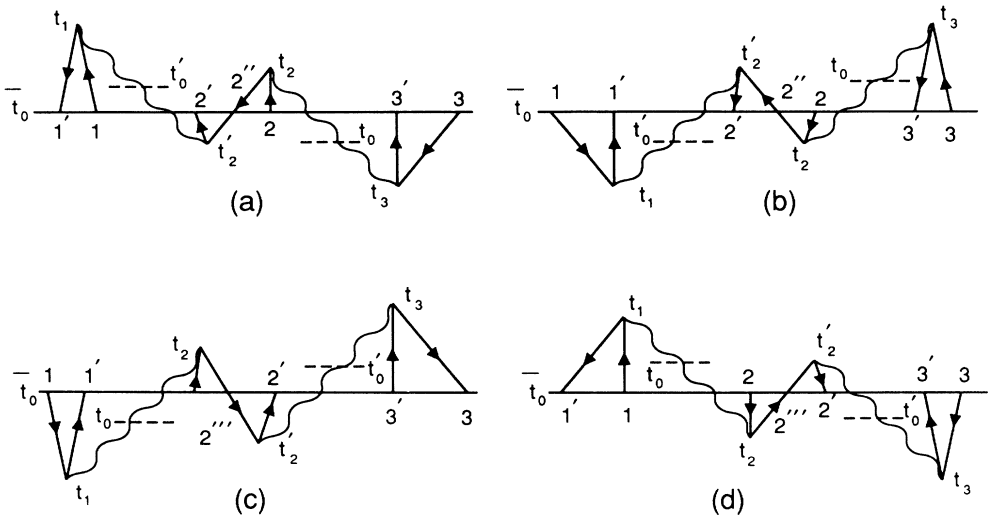


FIG. 9. Instantaneous three-body forces expressed in terms of folded diagrams. (a) and (c) are model-correcting, double-box folded diagrams, (b) and (d) are true-correcting double-box diagrams.

bases of these one-meson potentials, and the evaluation of this diagram requires that the time ordering of the dashed lines be as shown, which is the same as that of the corresponding one-meson potentials. Figure 8(c) is a true-correcting diagram, and it is needed because this time ordering is not generated by the iteration of Fig. 8(a). The true-correcting diagram is added to the potential. Details of the enumeration and evaluation of the diagrams can be found in Refs. 2, 3, and 10. We will give more details about the three-body folded-diagram force in Sec. IV B and in the Appendix.

Similar considerations lead to the three-body potentials in Fig. 9. The model-correcting diagram of Fig. 9(a) is subtracted as a separate term in the Hamiltonian because the iteration of the one-meson-exchange potential [Fig. 10(a)] generates (in addition to many allowed time orderings) these, which do not occur as part of the corresponding Feynman diagram, shown in Fig. 10(b). Each horizontal dashed line in Fig. 9(a), is, again, the time base of the corresponding one-meson-exchange potential [Fig. 8(a)] and is the time at which this potential occurs in all diagrams, including Fig. 10(a). Figure 9(b) is a true-correcting diagram, and it is added as a separate term in the potential because it is a time ordering of the original Feynman diagram, Fig. 10(b), that is not generated by the iterated one-meson-exchange potential in Fig. 10(a). The

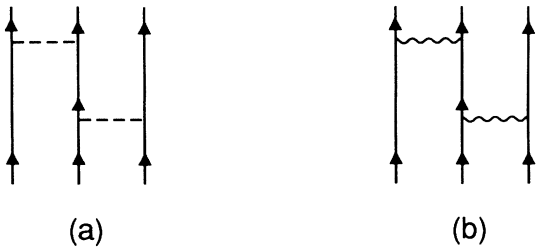


FIG. 10. Three-body processes contributing to the time-evolution operator $U(+\infty,-\infty)$. (a) diagrams expressed in terms of instantaneous potentials, (b) Feynman diagrams.

diagrams in Figs. 9(c) and (d) are model- and true-correcting diagrams, respectively, and these arise from processes similar to those in Figs. 10(a) and (b) but with the opposite sequence of interactions between the nucleons.

There are no zero-body contributions to the instantaneous interaction in the meson theory that we have been considering. We note that the number of diagrams is considerably smaller than that found in Figs. 4 and 5 because there are no hole lines to enlarge the set. In contrast to the case of the energy-dependent interaction, one may apply the familiar many-body (potential) theory to diagonalize the effective interaction $\overline{H}=H_0+\overline{H}_1$, since $\overline{H}_1$ is an instantaneous and Hermitian potential. The only complicating feature is that $\overline{H}_1$ has many-body terms, but the extension of familiar many-body theory in this regard is quite straightforward. For the energy of nuclear matter, we may apply Goldstone's linked-cluster expansion in its familiar form.

We emphasize a very interesting feature of this solution. For one thing, there are no medium modifications to the potential, so, for example, the same two-body interaction that is derived for free space is applicable to the many-body system, regardless of the number of particles. But again, as the number of particles increases, one must include forces acting simultaneously among an increasingly large number of nucleons. If this solution is to be practical, it is necessary that the many-body forces are not important. We show that in the case of the extrinsic three-body force, there are cancellations that make these contributions small.

We state a result, which is intuitively expected and which can be verified perturbatively; namely, that if we keep a complete set of single-particle states in the model space, the single-particle potential $u$ formally cancels out of the folded diagrams. The result is not surprising since $u$ was added and subtracted originally. Although we consider it to be a virtue that $\overline{H}_1$ does not depend on $u$, it may turn out in the future that one will want to use the

freedom of choosing $u$ to enhance the rate of convergence of the folded-diagram expansion.

Alternatively, we could use the results of Sec. 8 of Ref. 10 and define a potential in the situation that there are active holes. The Fermi surface $\epsilon_{FA}$ may be placed at some reference value, which may, for example, correspond to the value in normal nuclear matter, but the active orbitals would include the entire space, i.e., all particle and hole states of the nucleons. The folded-diagram rules then give the effective interaction among the particle and hole states. In this case also, the folded-diagram potential is completely connected, in contrast to the case for the energy-dependent interaction derived from Bloch and Horowitz, above. We have not pursued this option because it appears unnecessary for the purpose of this paper, but, after working through a few examples, we suspect that when due care is taken, this will be able to be cast back in the form derived from our original choice of model space.

### C. DISCUSSION

Note that we have arrived at quite different descriptions in the case of the instantaneous potential and energy-dependent interaction. In particular, for the instantaneous potential we make no medium modifications at all to the two- and three-body potentials. The two and three-body potentials in nuclear matter are just what they are in free space; in particular, there are no additional diagrams. The complete interaction through two-meson exchange is that shown in Figs. 8 and 9. One practical advantage of this procedure is that the two-body potential is fixed once and for all by the nucleon-nucleon phase shifts: one does not have to reevaluate it in nuclear matter for each density and energy. Other advantages are that there are fewer diagrams to evaluate and that the extrinsic three-body force is relative small (Sec. IV B).

One may wonder how things can be so simple in the approach through instantaneous potentials. How can one ignore the background potential $u_i$ and the Pauli principle?

Let us consider first the question of the background potential. A one-body potential is often added (and subtracted) to enhance the rate of convergence of perturbation theory. Since $u_i$ is added and subtracted, the final answer cannot depend on the choice of $u_i$ in principle. Whether or not it does in practice depends on how well the expansion has converged, which can only be answered by sufficient experience in numerical calculations. Actually, in the approach through instantaneous potentials, one does not give up the device of $u_i$, but rather one just employs it at a *later* stage of the calculation; namely, in applying the many-body theory to sum the potential interactions in the linked-cluster expansion. As we previously stated, it is possible to show perturbatively that even if $u_i$ is applied at the meson-theory level before the potential is defined, it tends to cancel out of the potential. This confirms our belief that we have not sacrificed an important degree of freedom by evaluating the nucleon-nucleon potential for nuclear matter in terms of the free-space nucleon energies.

Next consider the issue of the Pauli principle: can one really avoid excluding intermediate nucleon states with momentum $\epsilon_i < \epsilon_{FA}$ in Figs. 8 and 9? We remind the reader that the Pauli restriction does not, in general, have to be imposed explicitly in intermediate states provided antisymmetrized initial or final wave functions are used, and provided all Pauli-violating diagrams are kept: the Pauli-violating terms always appear in mutually canceling pairs. For the case at hand, the Pauli-violating pieces of the three-body forces in Fig. 9 cancel the Pauli-violating pieces in Fig. 8. We see, in particular, that some of the pieces of Figs. 9(a) and (c) (for example, those for which nucleons 1 and 3 are in the same state) cancel the unwanted pieces (those for which the state of an internal nucleon line lies within the Fermi sea) of the model-correcting diagrams of Fig. 8(b). Likewise, pieces of Figs. 9(b) and (d) cancel against the Pauli-violating pieces of the true-correcting diagram of Fig. 8(c). In this way we avoid having to apply the Pauli principle explicitly in intermediate states in the instantaneous potential.

One sees from the preceding discussion that there is a delicate interplay between the pieces of the two- and the three-body force. In particular, the three-body force is so closely associated with the uncrossed and crossed boxes from the two-body potential that one is not justified in using the full three-body force unless the complete two-meson-exchange two-body force is also evaluated. This somewhat subtle point is perhaps more evident in a diagrammatic than an algebraic approach.

## IV. THREE-BODY SYSTEM

There are two main reasons for bringing the three-body system into this discussion at this point. The first is that we want to evaluate some of the three-body forces shown in Sec. III to illustrate the methods discussed there in a somewhat abstract context. There have been many discussions of the intrinsic three-body force, but the extrinsic three-body force, which is the one relevant, for example, to the difference between the triton binding energy for energy-dependent and instantaneous potentials, has not been well studied. We therefore examine these in some detail.

Secondly, there have been extensive Faddeev calculations in the triton[15] with energy-dependent and energy-independent interactions, and we can use these results to support our assertion that the energy-dependent and energy-independent interactions give the same results when the many-body theory is carried to sufficiently high order.

### A. Three-body forces in the energy-dependent scheme

Consider first the extrinsic three-body force in the energy-dependent interaction. In this case, the three-body force is illustrated in Fig. 5(b). For an actual calculation, one needs to compute all eight of the time orderings, subject to the condition that each intermediate state contain at least one meson. (There are another eight diagrams in which the mesons interact with nucleons in the opposite time sequence.) One can easily convince oneself

that these eight diagrams are all coherent and generally nonvanishing. As it turns out, these were calculated on shell and in the nonrelativistic limit by Pask[17] and were reexamined more recently in Refs. 18 and 19. It was shown in the latter two works that this three-body force should be retained only in those calculations for which a complete relativistic treatment of the two-body potential has been made. It was furthermore shown that Pask incorrectly combined the various pieces of his calculation.

Although the discussion in Refs. 17–19 was motivated by different considerations, the results of these calculations are just what we need to estimate the extrinsic three-body force for the energy-dependent interaction in the present context. If nonrelativistic approximations are avoided in using the OBEPT′ interaction, which was the case in Ref. 15, then it is proper to add the three-body force of Fig. 5(b) (and the remaining legitimate time orders of it) to the results calculated with this two-body interaction.

### B. Three-body forces in the energy-independent scheme

Next, consider the three-body force in the instantaneous potential. The corresponding diagrams are given in Fig. 9, and we record some of the details of their evaluation in the Appendix. In this section we call attention to some of their salient features.

First, we recall the rule for evaluating the nucleon in these diagrams. All folded-nucleon lines propagate backward in time, and, of course, an ordinary nucleon line must propagate forward in time. A folded-nucleon line has the same propagator as a nucleon line that is not folded; namely,

$$e^{-iE_k\Delta t}\theta(\Delta t)=\frac{i}{2\pi}\int_{-\infty}^{+\infty}d\omega\frac{e^{-i\omega\Delta t}}{\omega-E_k+i\eta}\ , \tag{5}$$

where $\Delta t$ is the time difference between the beginning and the end of the line (as defined by the direction of the arrow). The complete value of a folded diagram is determined by integrating over all times subject to these time constraints and subject to the constraints that define the time base. We have found previously[2] that placing the time base at the average time of the diagram simplifies the structure of the higher-order terms, and so that is the way we fix the time base in this paper. Thus, for the one-meson-exchange terms, Fig. 8(a), the time base is fixed at $t_0=(t_1+t_2)/2$, where $t_1$ and $t_2$ are the times of absorption and emission of the meson. It is natural to place the time base in Fig. 9 at the average time as well, so we adopt the definition

$$\bar{t}_0=\frac{(t_1+t_2+t_2'+t_3)}{4}\ . \tag{6}$$

It is apparent from inspection of Fig. 9 that there is a large degree of cancellation between Figs. 9(a) and (d) and between Figs. 9(b) and (c) because of the similarity of their structure and because of the existence of the relative minus sign for the model- and true-correcting diagrams. Note that all lines in Fig. 9(a) are the same as the corresponding ones in Fig. 9(d), except those for nucleon 2. All time orderings of the vertices occuring at times $t_1$, $t_2,t_2'$, and $t_3$ are the same; in addition to the restrictions just mentioned, recall (from Sec. III B) that the time ordering of the time bases of the individual mesons must be maintained with respect to each other. The lines for nucleon 2 in Figs. 9(a) and (d) have the value

$$e^{-iE_2''(t_2'-t_2)}e^{-iE_2'(\bar{t}_0-t_2')}e^{-iE_2(t_2-\bar{t}_0)}\ . \tag{7}$$

The only difference between this in Figs. 9(a) and (d) is that $E$ has a different value in the two sets of diagrams [let these be $E_2''$ and $E_2'''$ in Figs. 9(a) and (d), respectively]. From this observation, it is easy to show that the diagrams are equal in magnitude but opposite in sign when

$$E_2+E_2'=E_2''+E_2'''\ . \tag{8}$$

When all external momenta can be neglected relative to the nucleon masses, this condition is satisfied and the three-body forces cancel identically. Moreover, if we use momentum eigenstates for our basis, the cancellation is exact when either $E_1'=E_1$ or $E_3'=E_3$.

A similar cancellation can be seen to occur between Figs. 9(b) and (c). Those cancellations are also apparent from the explicit expressions for the three-body force given in the Appendix. One also sees there that the sum of diagrams in Figs. 9(a) and (b) is a relativistic correction of order $(v/c)^2$. Likewise, the sum of Figs. 9(c) and (d) is of order $(v/c)^2$. Thus, the cancellation occurs between terms that are already quite small.

### C. Three-body results

There have been three-body calculations for the triton using the energy-dependent OBEPT (Ref. 15) and some variants (A,B,C) of the energy-independent, momentum-space potential OBEPQ.[16] These variants differ in the amount of $D$-state probability, ranging from 4.4% for model A to 5.6% for model C. Consequently, the triton binding-energy result is largest for model A (8.36 MeV) and reduces to 7.94 MeV for model C. Since our folded-diagram potential has a $P_D$ of 5.97%, a corresponding triton calculation is expected to yield about 7.8 MeV. This number has to compared with the result for OBEPT, which is 6.73 MeV according to Ref. 15. Thus, there is a sizable discrepancy of about 1 MeV, which shows that the many-body theories for energy-dependent and energy-independent potentials are inequivalent and that they are converging at different rates.

From the foregoing considerations we see that the main source of differences should be the extrinsic three-body force. Indeed, Pask[17] has estimated the extrinsic three-body force to be attractive and to contribute an additional binding of about $-1.03$ MeV to the triton. Although it has been pointed out[18,19] that Pask (incorrectly) adds this contribution to the energy calculated from an instantaneous potential, we have no reason to believe that he has incorrectly evaluated the three-body force. According to our analysis, this value corresponds to the size of the extrinsic three-body force in the energy-dependent interaction. Because of the cancellations between the model- and true-correcting folded diagrams discussed in Sec. IV B, we would conclude that the size of the extrin-

sic three-body force for the instantaneous potential would be small on this scale for the triton.

The excellent agreement that occurs between the two methods of calculation is consistent with our diagrammatic analysis, which shows that a sizable extrinsic three-body force occurs in the energy-dependent interaction but not in the energy-independent interaction. It also confirms our point that the same answer using energy-dependent and energy-independent interactions must be obtained when the calculation is carried out consistently. It would appear to be sufficient to carry out the calculation consistently through the two-meson-exchange level in order to find agreement between the two approaches.

## V. NUCLEAR-MATTER RESULTS

We can now compare the nuclear-matter results. We evaluate the two-body cluster of the Goldstone linked-cluster expansion using the standard Bethe-Goldstone equation with no potential acting on particle states. Just as in the case of the deuteron, the binding energy of nuclear matter is one of the observables that should be preserved by the effective interaction.[10] We see the binding energy per particle and the saturation Fermi momentum in Table II. The results of the calculation show that $BE/A = 20.7$ MeV for the energy-dependent, but only 11.3 MeV for the energy-independent interaction. These interactions correspond to the same meson-nucleon Lagrangian (apart from minor differences in the scalar coupling constants, see Table I), so they would correspond to the same $BE/A$ if the complete many-body theory were used for each, as in our previous study of the triton. Because $BE/A$ is not the same in the two cases, we conclude once more, for the case of infinite nuclear matter, that the energy-dependent and energy-independent interactions provide different descriptions in practice, with the corresponding expansions converging at different rates.

The differences in the numerical results can arise from (1) omission of three- (and higher-) body clusters, (2) omission of extrinsic three-body forces, and (3) omission of density-dependent pieces of the energy-dependent interaction. We are able to infer what the contribution of the extrinsic three-body forces and three-body clusters give for the instantaneous potential. The three- (and many-) body linked-cluster contributions to $BE/A$ have been calculated by Day in Ref. 20 for a series of instantaneous potentials. We see from his results that the many-body cluster corrections give an additional attraction of about 5 MeV. Our own results show that, to first approximation, the extrinsic three-body force in the instantaneous potential does not contribute to nuclear matter. Putting this together, we would conclude that the nuclear-matter $BE/A$ in the instantaneous potential scheme, including two-body plus three-body clusters, would be about 16.3 MeV/nucleon.

There have been no calculations (to our knowledge) of the three-body cluster contribution in infinite nuclear matter corresponding to the energy-dependent force. We infer from our numerical values of $BE/A$ for the two cases that the sum of all corrections for this interaction would have to be *repulsive* by about $20.7-16.3=4.4$ MeV/nucleon in order to bring the instantaneous and energy-dependent interaction results into agreement.

On the one hand, the results of Ref. 20 suggest that the many-body clusters give an attractive contribution, because that is what is found for all interactions considered there. However, the three-body calculations of Ref. 15 give support for the idea that the two- plus three-body effects are repulsive for the energy-dependent interaction. These calculations give $BE/A = 6.73$ MeV for the energy-dependent interaction in the triton and $BE/A \sim 7.8$ MeV for the corresponding instantaneous potential. Unfortunately, it is not easy to break this calculation down into a two-body and a three-body cluster contribution, so we cannot tell whether the repulsion in the energy-dependent calculation comes from the three- or from the two-body terms. We conclude that it is necessary to do the three- and many-body cluster calculations explicitly for the energy-dependent potential.

The extrinsic three-body forces are attractive, at least for the triton. In nuclear matter, the situation is a bit more complicated than in the case of the triton, because we now have three-body diagrams with intermediate hole states, for example Fig. 5(c). Thus, there will be some terms with positive signs and some with negative signs, leading to density-dependent cancellations in the many-body problem. We must also recall that there are additional density-dependent corrections to the two-body force itself [e.g., Figs. 4(d)–(g)] that have not ever been considered and that may modify the solution of the Bethe-Goldstone equation.

Of course, one cannot forget the two-meson-exchange diagrams of Figs. 3(f) and (g), which have never been calculated. A lot more work is required in the case of the energy-dependent interaction to complete a consistent nuclear-matter calculation through the level of two-meson exchange.

## VI. DISCUSSION AND CONCLUSIONS

In an earlier paper, we showed that the nucleon-nucleon phase shifts are essentially identical for the energy-dependent interaction and its corresponding instantaneous potential, implying a rapid convergence of the corresponding expansion for the potential in the two-body problem. In contrast, we found here that when the same potentials are used in a nuclear-matter calculation, the particular equivalence found for two free nucleons no longer holds. Specifically, $BE/A$ for nuclear matter, obtained by truncating the Goldstone expansion at the two-body linked-cluster level, is quite different for the two forms of interaction.

If the many-body theory is carried to all orders, one should obtain the same $BE/A$ because these interactions correspond to the same meson-nucleon Lagrangian. The validity of this assertion was confirmed here by combining Faddeev calculations in the triton[15] for energy-dependent and corresponding energy-independent interactions and a three-body force calculation by Pask.[17] In this case, the practical equivalence in the three-body problem is thus restored by the extrinsic three-body force

(an extrinsic three-body force has been defined here as one arising from the specific treatment of retardation at the two-body level).

Some of the discrepancies in our nuclear matter results are presumably explained by three- (and higher-) body linked clusters. Our formal examination of the many-body theory shows that nontrivial differences between the two cases exist. We have argued that the extrinsic three-body forces and density-dependent corrections are especially important for the energy-dependent interaction.

We were able to estimate the size of the higher-order linked clusters [5 MeV/nucleon (Ref. 20)] and the extrinsic three-body forces (0 MeV/nucleon) corresponding to the case of the instantaneous potential, giving a net binding of 16.3 MeV/nucleon. The three-body force is small because of the results found in Sec. IV C that there is a high degree of cancellation among the pieces of the extrinsic three-body force in the instantaneous potential.

We were unable to make the necessary estimates for the energy-dependent potential, hence it is not possible to completely reconcile the differences in the nuclear-matter results at the present time. At the two-body level, our solution of the Bethe-Goldstone equation according to the recipe of Ref. 8 gives 20.7 MeV for the energy-dependent interaction. Based on our expectation that BE/$A$ must be the same for the energy-dependent and energy-independent calculations, we conclude that all remaining corrections will be repulsive by at least 4 MeV.

The three-body linked clusters have not been calculated for the energy-dependent interaction. We have given, in diagrammatic form in Sec. IV of this paper, the additional ingredients that one should consider in order to make a complete calculation for the energy-dependent interaction. A numerical calculation of the three-body cluster and the various many-body corrections based on the energy-dependent interaction is needed to confirm the conclusions that we come to here.

One cannot forget that agreement between the empirical value of BE/$A$ and theory requires more physics than we have discussed in this paper. For example, there are the intrinsic three-body forces and the possibility of relativistic effects involving the negative-energy sector[21] that we have omitted. Considering the ultimate complexity of a complete theory, it is of some importance to find the simplest approach to the conventional part of the many-body problem, which has been the aim of this paper.

We conclude that the most reliable estimate of BE/$A$ for the three-body system and infinite nuclear matter has been obtained for instantaneous potentials. The energy-dependent interactions suffer from the drawback that associated with them are non-negligible extrinsic three-body forces and numerous density-dependent corrections. These have never been evaluated. It would be interesting to see a consistent calculation of BE/$A$ through the two-meson-exchange level for density-dependent potentials.

## ACKNOWLEDGMENTS

One of use (M.B.J.) would like to acknowledge the hospitality of J. Speth and the Institut für Kernphysik (IKP) of the Forschungszentrum Jülich G.m.b.H. (KFA). The work was supported in part by the Humboldt Foundation and the U. S. Department of Energy. Thanks are due to T. Hippchen for computational help.

## APPENDIX A: TIME INTEGRATIONS FOR FIG. 9

As in Ref. 2, we write the value of a folded diagram as a vertex contribution that is the same for all four diagrams in Fig. 9 and a propagator contribution $J^{\alpha}$. The propagator contribution consists of an internal part $W^{\alpha}(t_1 t_2' t_2 t_3)$ and a part for the external nucleon lines, where $\alpha=(a,b,c,d)$ corresponds to Figs. 9(a)–(d), respectively. The rules for evaluating the diagrams are given in Sec. III of Ref. 2. The function $W^{\alpha}$ may be written in the form

$$W^{\alpha}(t_1 t_2' t_2 t_3)=\left[\frac{1}{2\pi}\right]^4 \int d\nu_1 d\nu_2' d\nu_2 d\nu_3 e^{-it_1\nu_1} e^{-it_2'\nu_2'} e^{-it_2\nu_2} e^{-it_3\nu_3} (2\pi)\delta(\nu_1+\nu_2'+\nu_2+\nu_3) w^{\alpha}(\nu_1\nu_2'\nu_2\nu_3) , \tag{A1}$$

where the delta function expresses invariance with respect to time translations. The external legs in each case contribute

$$e^{-i\Delta E_1(\bar{t}_0-t_1)} e^{-iE_2'(\bar{t}_0-t_2')} e^{iE_2(\bar{t}_0-t_2)} e^{-i\Delta E_3(\bar{t}_0-t_3)} , \tag{A2}$$

where $\Delta E_j=E_{\text{out}}-E_{\text{in}}$, with $E_{\text{out}}$ ($E_{\text{in}}$) being the single-particle energy of the line leaving (entering) the vertex at time $t_j$ and $\bar{t}_0$ is the time base of the three-body force. The time base is fixed according to Eq. (6). The value $J^{\alpha}$ is found by integrating over all times subject to this constraint. We then have, following the straightforward calculation similar to that in Appendix B of Ref. 2,

$$J^{\alpha}=iw^{\alpha}(\Delta E_1-\Delta E/4, E_2'-\Delta E/4, -E_2-\Delta E/4, \Delta E_3-\Delta E/4) , \tag{A3}$$

where

$$\Delta E=\Delta E_1+E_2'-E_2+\Delta E_3 . \tag{A4}$$

It now remains to calculate $w^{\alpha}(\nu_1,\nu_2',\nu_2,\nu_3)$. The ingredients are the internal nucleon, the meson propagators, and the time constraints that maintain the proper time orderings of the time bases represented by the horizontal dashed lines in Fig. 9. The meson propagators are

$$\frac{1}{2\pi}\int_{-\infty}^{+\infty} d\omega \frac{e^{-i\omega\Delta t}}{\omega^2-e_q^2+i\eta} , \tag{A5}$$

where $e_q=(q^2+m^2)^{1/2}$ is the energy of a meson, and the nucleon propagator is given by Eq. (5), where $E_k=E_2''$ for Figs. 9(a) and (b) and $E_k=E_2'''$ for Figs. 9(b) and (d). Time orderings are maintained for the time bases by using the integral representations for the theta functions; for example, the restriction that $t_0'>t_0$ in Fig. 9(a) is

$$\theta(t_0'-t_0)=\frac{1}{2\pi}\int_{-\infty}^{+\infty} d\bar{\omega}\frac{e^{-i\bar{\omega}(t_0'-t_0)}}{\bar{\omega}+i\eta} . \tag{A6}$$

Putting together the various propagators and time restrictions, we find

$$W^a(t_1t_2't_2t_3)=\left[\frac{i}{2\pi}\right]^4\int d\omega_{12}d\omega_{23}d\omega\, d\bar{\omega}\frac{e^{-i\omega_{12}(t_1-t_2')}}{\omega_{12}^2-e_{12}^2+i\eta}\frac{e^{-i\omega_{23}(t_2-t_3)}}{\omega_{23}^2-e_{23}^2+i\eta}\frac{e^{-i\omega(t_2'-t_3)}}{\omega-E_2''-i\eta}\frac{e^{-i(\bar{\omega}/2)(t_1+t_2'-t_2-t_3)}}{\bar{\omega}+i\eta} , \tag{A7a}$$

$$W^b(t_1t_2't_2t_3)=-\left[\frac{i}{2\pi}\right]^4\int d\omega_{12}d\omega_{23}d\omega\, d\bar{\omega}\frac{e^{-i\omega_{12}(t_1-t_2')}}{\omega_{12}^2-e_{12}^2+i\eta}\frac{e^{-i\omega_{23}(t_2-t_3)}}{\omega_{23}^2-e_{23}^2+i\eta}\frac{e^{-i\omega(t_2'-t_3)}}{\omega-E_2''-i\eta}\frac{e^{-i(\bar{\omega}/2)(t_1+t_2'-t_2-t_3)}}{\bar{\omega}-i\eta} . \tag{A7b}$$

A similar calculation for Figs. 9(c) and (d) reveals that

$$W^c(t_1t_2't_2t_3)=-W^b(t_1t_2t_2't_3)|_{E_2''\to -E_2'''} , \tag{A8a}$$

$$W^d(t_1t_2't_2t_3)=-W^a(t_1t_2t_2't_3)|_{E_2''\to -E_2'''} , \tag{A8b}$$

so we need only calculate the integrals in Eqs. (A7a) and (A7b).

If we now change variables in Eq. (A7a) as follows,

$$\begin{aligned} \nu_1&=\omega_{12}+\bar{\omega}/2 ,\\ \nu_2'&=-\omega_{12}+\omega+\bar{\omega}/2 ,\\ \nu_2&=\omega_{23}-\omega-\bar{\omega}/2 ,\\ \nu_3&=-\omega_{23}-\bar{\omega}/2 , \end{aligned} \tag{A9}$$

then we find Eq. (A1) to hold with

$$w^a(\nu_1\nu_2'\nu_2\nu_3)=\int\frac{d\omega}{2\pi}\frac{1}{\frac{1}{4}(\nu_1-\nu_2'+\omega)^2-e_{12}^2+i\eta}\frac{1}{\omega-E_2''-i\eta}\frac{1}{\frac{1}{4}(\nu_2-\nu_3+\omega)^2-e_{23}^2+i\eta}\frac{1}{\nu_1+\nu_2'-\omega+i\eta} . \tag{A10}$$

We now easily see

$$w^b(\nu_1\nu_2'\nu_2\nu_3)=-\int\frac{d\omega}{2\pi}\frac{1}{\frac{1}{4}(\nu_1-\nu_2'+\omega)^2-e_{12}^2+i\eta}\frac{1}{\omega-E_2''+i\eta}\frac{1}{\frac{1}{4}(\nu_2-\nu_3+\omega)^2-e_{23}^2+i\eta}\frac{1}{\nu_1+\nu_2'-\omega-i\eta} , \tag{A11}$$

and from Eq. (A8)

$$\begin{aligned} w^c(\nu_1\nu_2'\nu_2\nu_3)&=-w^b(\nu_1\nu_2\nu_2'\nu_3)|_{E_2''\to -E_2'''} ,\\ w^d(\nu_1\nu_2'\nu_2\nu_3)&=-w^a(\nu_1\nu_2\nu_2'\nu_3)|_{E_2''\to -E_2'''} . \end{aligned} \tag{A12}$$

We now evaluate Eqs. (A10) and (A11) by closing the contour in the lower $\frac{1}{2}$ plane. The poles in Eq. (A10) come from the meson propagators only, but in Eq. (A11) they come from all four propagators. However, since the integrands are the same except for the infinitesimals in the nucleon propagators, and these integrals have a relative minus sign, the two poles from the meson propagators cancel out. The final result picks up all of its contribution from the second and fourth energy denominator in Eq. (A11). Thus, we find

$$w^a(\nu_1\nu_2'\nu_2\nu_3)+w^b(\nu_1\nu_2\nu_2'\nu_3)=[-(-2\pi i)]\left[\frac{1}{\frac{1}{4}(\nu_1-\nu_2'+E_2'')^2-e_{12}^2}\frac{1}{\frac{1}{4}(\nu_2-\nu_3+E_2'')^2-e_{23}^2}\frac{1}{\nu_1+\nu_2'-E_2''}\right.$$

$$\left.-\frac{1}{\nu_1^2-e_{12}^2}\frac{1}{\nu_1+\nu_2'-E_2''}\frac{1}{\nu_3^2-e_{23}^2}\right] . \tag{A13}$$

The structure is a bit more transparent if we define

$$D''=E_2''-\nu_1-\nu_2'=E_2''+\nu_2+\nu_3\ . \tag{A14}$$

Then,

$$w^a+w^b=-\frac{2\pi i}{D''}\left[\frac{1}{(D''/2+\nu_1)^2-e_{12}^2}\times\frac{1}{\frac{1}{4}(D''/2-\nu_3)^2-e_{23}^2}-\frac{1}{\nu_1^2-e_{12}^2}\frac{1}{\nu_3^2-e_{23}^2}\right]. \tag{A15}$$

From Eq. (A15) it is clear that $w^a+w^b$ is finite in the limit that $D''\to 0$, so we do not have any worry about singularities in the three-body force (one can show that $w^a$ and $w^b$ are separately finite in the same sense). Namely, if we rearrange, we find

$$w^a+w^b=2\pi i\left[\frac{D''/4+\nu_1}{(D''/2+\nu_1)^2-e_{12}^2}\frac{1}{\nu_1^2-e_{12}^2}\frac{1}{\nu_3^2-e_{23}^2}-\frac{1}{(D''/2+\nu_1)^2-e_{12}^2}\times\frac{D''/4-\nu_3}{(D''/2-\nu_3)^2-e_{23}^2}\frac{1}{\nu_3^2-e_{13}^2}\right] \tag{A16}$$

and, using Eq. (A12), we find for $w^c+w^d$

$$w^c+w^d=-2\pi i\left[\frac{D'''/4+\nu_1}{(D'''/2+\nu_1)^2-e_{12}^2}\frac{1}{\nu_1^2-e_{12}^2}\frac{1}{\nu_3^2-e_{23}^2}-\frac{1}{(D'''/2+\nu_1)^2-e_{12}^2}\times\frac{D'''/4-\nu_3}{(D'''/2-\nu_3)^2-e_{23}^2}\frac{1}{\nu_3^2-e_{13}^2}\right], \tag{A17}$$

where

$$D'''=E_2'''-\nu_1-\nu_2=-E_2'''+\nu_2'+\nu_3\ . \tag{A18}$$

It is clear from the definitions of $D''$ and $D'''$ that the expressions in Eqs. (A16) and (A17) become equal and opposite when

$$E_2''-E_2=-E_2'''+E_2'\ , \tag{A19}$$

which is the same as the condition in Eq. (8). Note that the set of folded diagrams in Figs. 9(a) and (b) and 9(c) and (d) are individually of order $(v/c)^2$, but that, even then, these corrections vanish in the limit of Eq. (A19). The complete propagator contribution for the three-body force $\sum_\alpha J^\alpha$ is now obtained by adding Eqs. (A16) and (A17), and using Eq. (A3).


[1] R. Machleidt, K. Holinde, and Ch. Elster, Phys. Rep. **149**, 1 (1987).

[2] M. B. Johnson, Ann. Phys. (NY) **97**, 400 (1976).

[3] K. Holinde, M. B. Johnson, and R. Machleidt, Phys. Rev. C **32**, 1 (1985).

[4] H. A. Bethe, Annu. Rev. Nucl. Sci. **21**, 93 (1971).

[5] H. J. Zuilhof and J. A. Tjon, Phys. Rev. C **24**, 736 (1981); Th. Hippchen and K. Holinde, *ibid.* **37**, 239 (1988).

[6] M. Chemtob and M. Rho, Nucl. Phys. **A163**, 1 (1971).

[7] B. Desplanques, Phys. Lett. B **203**, 200 (1988).

[8] D. Schuette, Nucl. Phys. **A221**, 450 (1974).

[9] C. Bloch and J. Horowitz, Nucl. Phys. **8**, 91 (1958).

[10] M. B. Johnson and M. Baranger, Ann. Phys. (NY) **62**, 172 (1971).

[11] B. H. Brandow, Rev. Mod. Phys. **39**, 771 (1967); in *Lectures in Theoretical Physics,* edited by K. T. Mahanthappa (Gordon and Breach, New York, 1969), Vol. 11.

[12] K. Holinde, Nucl. Phys. **A328**, 439 (1979); R. Machleidt and K. Holinde, *ibid.* **A350**, 396 (1980).

[13] A. Picklesimer, P. C. Tandy, and R. M. Thaler, Ann. Phys. (N.Y.) **145**, 207 (1983).

[14] K. Brueckner, in *The Many-Body Problem,* edited by C. DeWitt (Wiley, New York, 1959), p. 47.

[15] R. A. Brandenburg, G. S. Chulick, R. Machleidt, A. Picklesimer, and R. Thaler, Phys. Rev. C **38**, 1397 (1988).

[16] R. A. Brandenburg, G. S. Chulick, R. Machleidt, A. Picklesimer, and R. M. Thaler, Phys. Rev. C **37**, 1245 (1988).

[17] C. Pask, Phys. Lett. **25B**, 78 (1967).

[18] S.-N. Yang and W. Gloeckle, Phys. Rev. C **33**, 1774 (1986).

[19] S. A. Coon and J. L. Friar, Phys. Rev. C **34**, 1060 (1986).

[20] B. D. Day, Phys. Rev. Lett. **47**, 226 (1981); Phys. Rev. C **24**, 1203 (1981).

[21] M. R. Anastasio, L. S. Celenza, W. S. Pong and C. M. Shakin, Phys. Rep. **100**, 327 (1983).